JMEPEG (2018) 27:5124–5129
https://doi.org/10.1007/s11665-018-3599-9

1059-9495/$19.00

Influence of Thermal History on the Hot Ductility of a Continuously Cast Low Alloyed Cr-Mo Steel

C. Hoflehner, S. Ilie, J. Six, C. Beal, and C. Sommitsch

(Submitted October 31, 2017; in revised form July 18, 2018; published online August 29, 2018)

The hot ductility of a low alloyed Cr-Mo steel has been investigated to evaluate the surface cracking sensitivity within the straightening or unbending regime during the continuous casting process. Tensile samples were subjected to various thermal treatments, including melting and solidification, and were tested at deforming temperatures ranging between 600 and 1100 °C using a strain rate of 10^{-3} s^{-1}. Hot ductility was evaluated based on reduction in area measurement and metallographic investigations. The investigated steel exhibits a drop in ductility at around 800 °C due to intergranular cracking. Microstructural examinations and supplementary thermokinetic computer simulations were carried out to describe the evolution of the microstructure during solidification and cooling.

Keywords casting and solidification, microscopy, optical metallography, segregation, steel

1. Introduction

During the straightening operation in continuous casting, the steel slab is subjected to high mechanical as well as thermal stresses. This may cause surface and internal tears that can lead to a loss of product yield and quality (Ref 1-4). The sensitivity of continuously cast steels to transverse cracking can be primarily addressed to the poor hot ductility at temperatures between 700 and 1000 °C; this is the temperature range where the straightening operation takes place (Ref 5). The reason for the poor ductility can be found in the strain concentrations at the ferrite films along the austenite grain boundaries and precipitations. Ferrite, which preferentially forms at the austenite grain boundaries, has a lower strength than austenite and strain is concentrated in the low strength phase (Ref 6). Also, a high amount of fine precipitations leads to local precipitation hardening with severe stress concentrations, thus triggering the nucleation of wedge-type cavities as well as favoring interconnection of cavities surrounding the precipitates (Ref 7).

To evaluate the hot ductility of steels, hot tensile testing of samples using similar thermomechanical conditions and measuring the percentage reduction in area after fracture (RA) has proved to be an effective method (Ref 8, 9). This RA value should exceed the limit of 40% to avoid transverse cracks (Ref 10). A realistic approach to simulate the thermomechanical conditions of continuous casting is to use in situ melted and solidified specimens. This considers the segregation of alloying elements at grain boundaries and allows the dissolution and nucleation of certain particles, such as MnS or TiN that weaken the grain boundary (Ref 11-13).

In the present work, the hot ductility of a low alloyed C-Cr-Mo-Mn-Si steel in a temperature range of 600-1200 °C was investigated to predict the temperatures at which the materials' ductility deteriorates.

This article is an invited submission to JMEP selected from presentations at the Symposium "Steel Making," belonging to the Topic "Processing" at the European Congress and Exhibition on Advanced Materials and Processes (EUROMAT 2017), held September 17-22, 2017, in Thessaloniki, Greece, and has been expanded from the original presentation.

C. Hoflehner, C. Beal, and **C. Sommitsch**, Institute of Materials Science, Joining and Forming, Graz University of Technology, Graz, Austria; and **S. Ilie** and **J. Six**, Voestalpine Stahl Linz GmbH, Linz, Austria. Contact e-mail: christian.hoflehner@tugraz.at.

2. Experimental

The chemical composition of the investigated steel is given in Table 1. Thermodynamic equilibrium calculations have been performed to obtain phase transformation temperatures using the thermokinetic software MatCalc (version 6.00) (Ref 14). Here, the ferrite start temperature (A_{e3}) was found to be 857 °C and the ferrite finish temperature (A_{e1}) 763 °C.

The hot tensile tests were conducted on an in-house developed thermomechanical simulator BETA 250-5 as shown in Fig. 1(a). The experiments were carried out in a fine vacuum atmosphere and with the use of an inductive heating system. Cylindrical tensile samples were machined from the cast and hot-rolled billet with their axis parallel to the rolling direction. The dimensions of the tensile samples are shown in Fig. 1(b). One end of the specimen was screwed into the upper crosshead, which is responsible for the displacement. The lower end was clamped on a special extractor, which has a fixed position and is equipped with a steel spring and three gripper arms. This lower extractor unit has three functions; it compensates for the thermal expansion downwards, it holds the sample when pulling it upwards and supports the specimen when it is in the mushy state; so it does not break under its own bodyweight in this unstable condition. A Pt/Pt-Rh thermocouple was spot-welded to the body center of the specimen to measure the surface temperature during the experiment.

Figure 2 shows a sketch of the temperature cycle, which was used for the investigation. The measured surface temperature reached a maximum of 1440 °C during the melting phase, at which the samples were hold for 60 s. Directly after melting,

Table 1 Chemical composition of the investigated steel (wt.%)

C	Cr	Mo	Mn	Si	Al	Ni	N	P	S	Ti
0.15	1.49	0.59	0.635	0.64	0.037	0.023	39 ppm	0.0036	0.0014	0.003

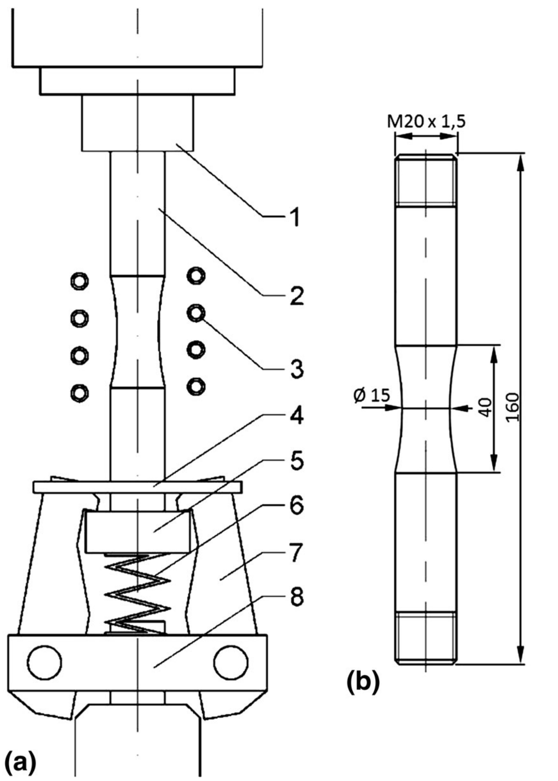

Fig. 1 (a) Tensile testing equipment "BETA 250-5" (1. tension arm, 2. tensile specimen, 3. induction coil, 4. securing ring, 5. holding ring, 6. steel spring, 7. gripper arm, 8. extractor unit); (b) geometry and dimension of the tensile sample (Ref 15)

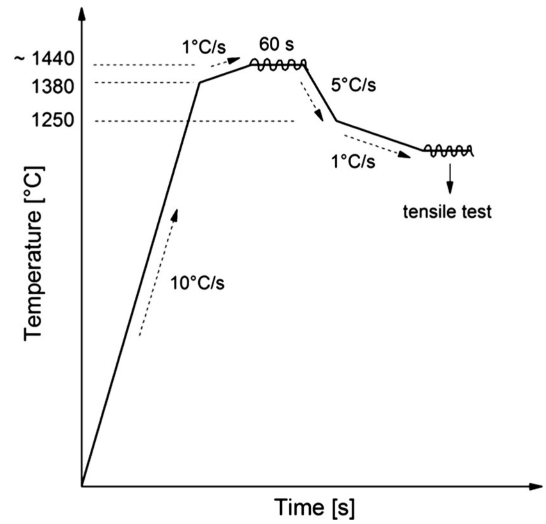

Fig. 2 Temperature cycle for the experiment

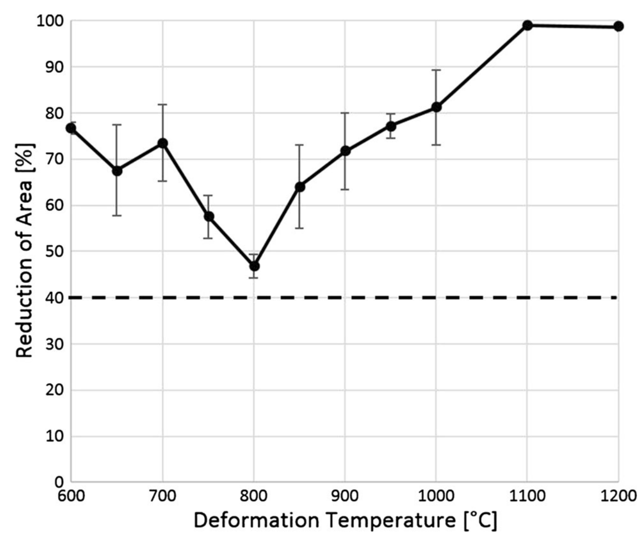

Fig. 3 Hot ductility curve

the specimens were cooled with 5 °C s^{-1} to 1250 °C and further with 1 °C s^{-1} to testing temperatures between 600 and 1200 °C. All tensile tests were performed at a strain rate of 1×10^{-3} s^{-1}. After tensile testing, the hot ductility was evaluated by graphically measuring the reduction in area at a stereo microscope. For every testing temperature, a total number of three samples were tested. Due to the formation of solidification shrinkages and therefore the reduction in the load-bearing cross section through the melting process, the area of these cavities was subtracted from both the initial cross section and the cross section after fracture. Metallographic analyses were carried out on longitudinally sectioned specimens near their fracture surface using light optical microscopy (LOM) and scanning electron microscopy (SEM).

3. Result and Discussion

3.1 Hot Ductility

The hot ductility curve of the in situ melted steel is presented in Fig. 3. The ductility trough ranges from 750 to 850 °C with a minimum at 800 °C. A ductility trough is characterized by a severe decrease in ductility in a certain temperature range. Above 900 °C, in the single-phase austenite region, the steel showed a better ductility behavior. At lower temperatures below 700 °C, however, the ductility recovers. The critical proposed RA value of 40% by Mintz is drawn as a horizontal dashed line as well. Despite the poor ductility behavior at the deformation temperature of 800 °C, the RA values of this steel never go below this critical line.

3.2 Metallography

Figure 4 shows a SEM image of the fracture surface of a ruptured specimen after tensile testing at deformation temperature of 800 °C, which revealed distinct intergranular cracking. At a deformation temperature of 700 °C, the surface showed a

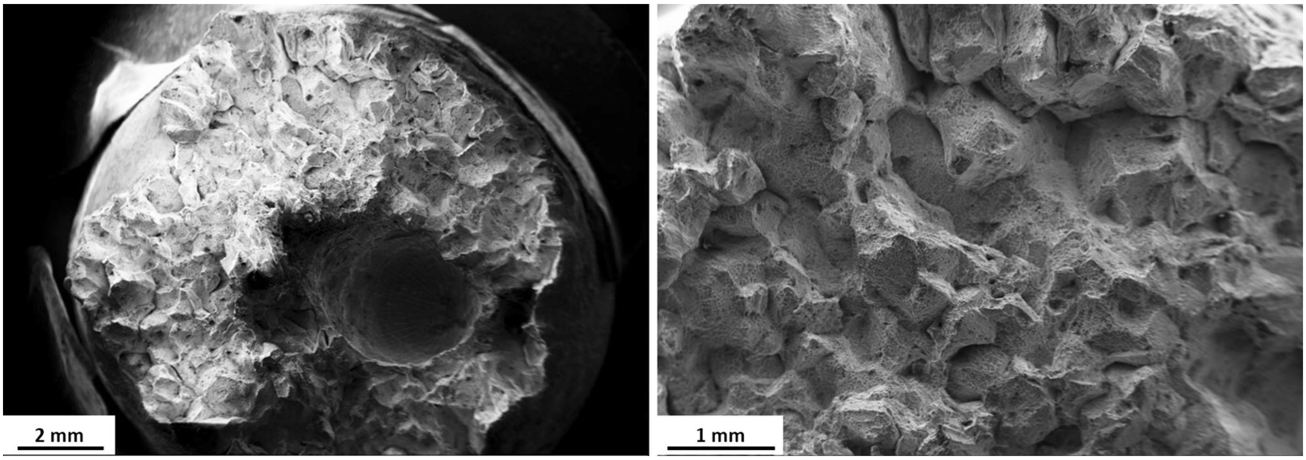

Fig. 4 SEM images of samples strained to rupture at a strain rate of 10^{-3} s^{-1} at 800 °C showing primarily intergranular fracture and coarse grains

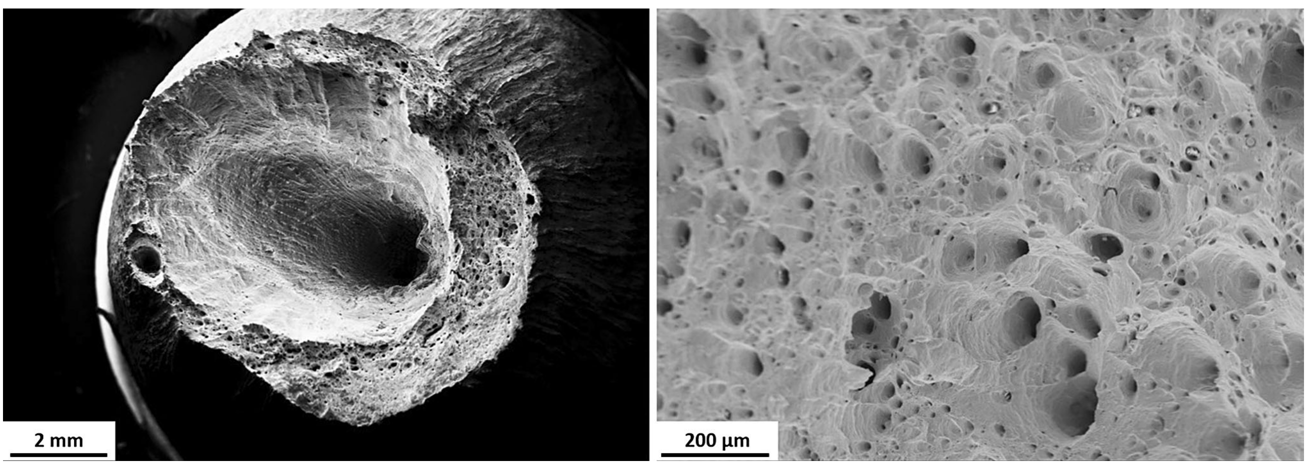

Fig. 5 SEM images of samples strained to rupture at a strain rate of 10^{-3} s^{-1} at 700 °C showing a ductile fracture surface

ductile fracture as shown in Fig. 5. Moreover, extensive solidification shrinkage holes, as seen in Fig. 4 and 5, were observed on the fracture surface due to the preceding melting process, which accelerated the materials decohesion if a stress was applied.

Figure 6 shows LOM images of longitudinal sections of water-quenched specimens after pulling to fracture. At a deformation temperature of 900 °C, first small islands of ferrite were observed, as seen in Fig. 6(a). At a deformation temperature of 850 °C, the number of ferrite islands increased, as seen in Fig. 6(b). At a deformation temperature of 800 °C (ductility minimum), the formation of ferrite films along the prior austenite grain boundaries can be observed, as seen in Fig. 6(c). A crack forming within thin bands of ferrite can also be observed. At a deformation temperature of 750 °C, the amount of ferrite increased, as seen in Fig. 6(d). In a study analyzing the hot ductility of steel using a micro–macromodel approach (Ref 16), it was found that the ferrite networks caused a large drop in ductility explaining the lower ductility seen in the two-phase region in the steel material.

The matrix consists of regions of upper and lower bainite and regions of martensite, which was confirmed by microhardness testing. In comparison with the LOM images of a specimen, which was quenched after tensile testing at 800 °C (Fig. 7a), the LOM image of a specimen, which was quenched without tensile testing, does not show these thin bands of ferrite, as seen in Fig. 7(b). This indicates that, at this temperature, the ferrite in the tensile specimen is deformation induced. In both cases, bright spots were found, which are marked by black arrows in Fig. 7. Microhardness measurements showed that these bright spots have a hardness of 515 HV0.01. These bright, hard spots appear to be the result of the segregation of substitutional alloying elements during dendritic solidification. The addition of elements like manganese, chromium and molybdenum causes solidification to occur over a range of temperatures and compositions. The dendritic cores solidify as relatively pure metal while the interdendritic spaces become enriched in solute. The literature studies (Ref 17-19) have shown Mn to be the alloying element most responsible for carbon segregation. Voldrich (Ref 20) showed that carbon migrates from low- to high-Mn regions during cooling. Manganese stabilizes austenite and lowers the A_{r3} temperature. During cooling, ferrite forms in regions with a high A_{r3} temperature and rejects carbon into the austenite of adjacent low-A_{r3} regions, resulting in the formation of carbon-rich and carbon-depleted regions.

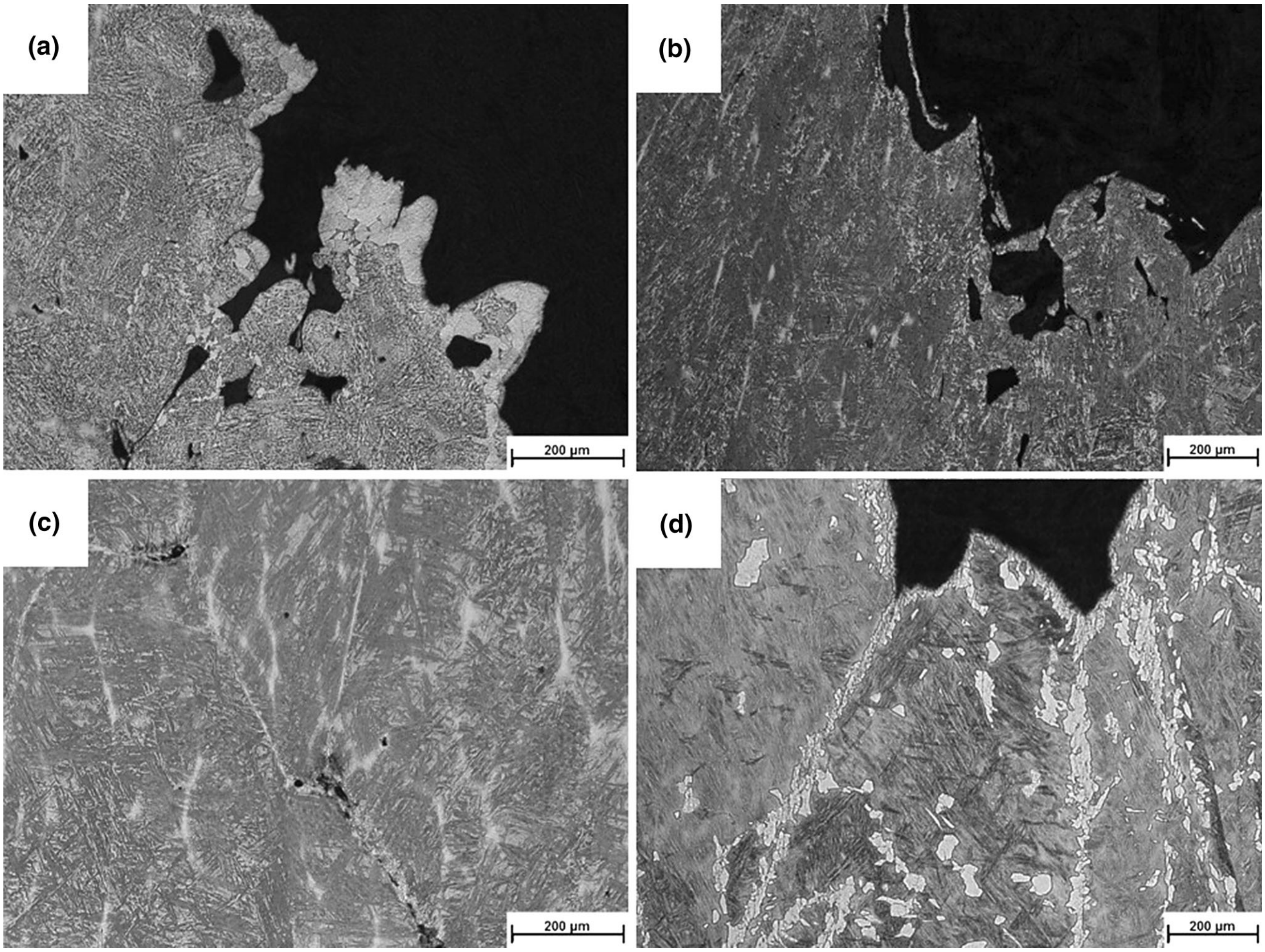

Fig. 6 LOM images of a water-quenched specimen, etched with 3% Nital for 10 s at a (a) testing temperature of 900 °C, (b) testing temperature of 850 °C, (c) testing temperature of 800 °C and (d) testing temperature of 750 °C

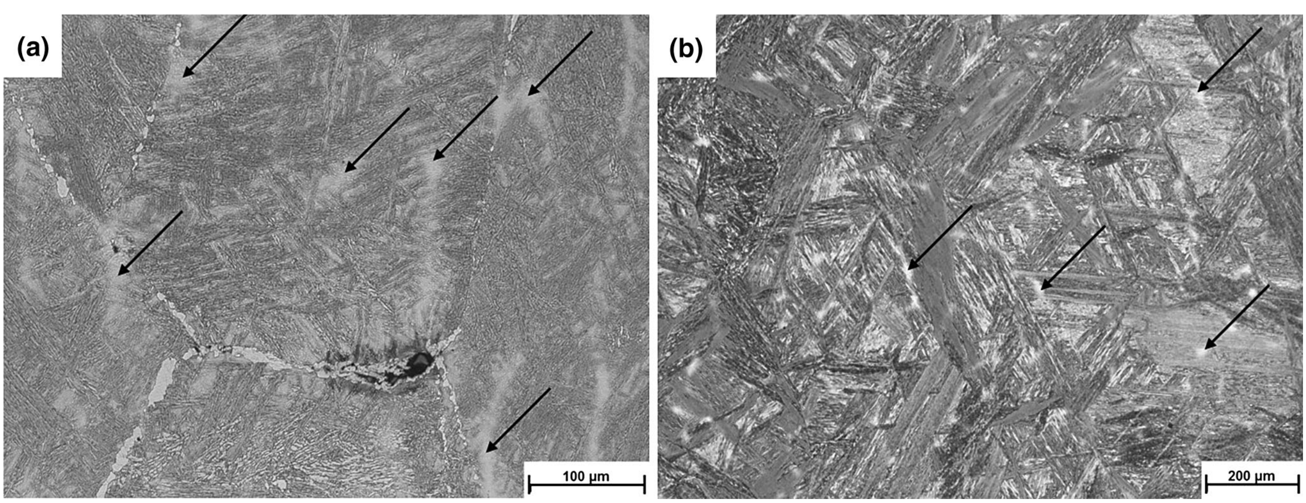

Fig. 7 LOM images of water-quenched specimen, etched with 3% Nital for 10 s. (a) Pulled to fracture, initial crack in thin ferrite bands, testing temperature 800 °C, RA = 46.8%. (b) Same temperature cycle as in (a), but without tensile test

EDX measurements show the difference in the chemical composition between a high solute region and a low solute region. Figure 8 shows a SEM image of a water-quenched specimen which was pulled at a testing temperature of 800 °C. Spot 1 is a low solute region within a ferrite film and Spot 2 marks a high solute region. The difference in the chemical

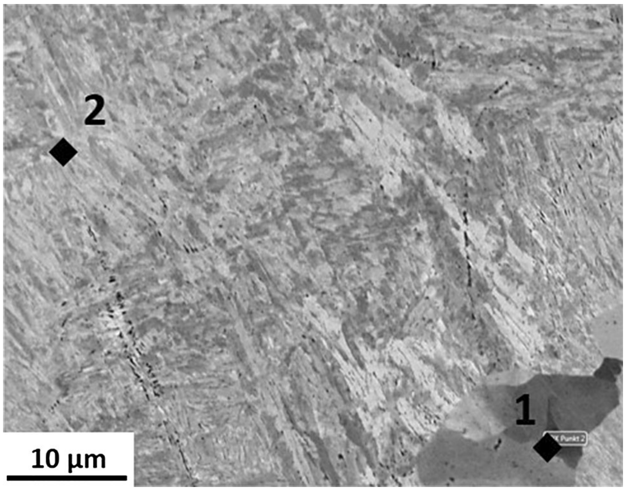

Fig. 8 SEM image of a water-quenched specimen, pulled at testing temperature of 800 °C; spot 1: low solute- region; spot 2 high solute region

Table 2 EDX measurement of a low solute and a high solute region

Spot	Mn Weight, %	Mo Weight, %	Cr Weight, %	Si Weight, %
1	0.56	0.36	1.24	0.61
2	0.96	0.78	1.69	0.75

composition between these two spots is given in Table 2. Spot 2 shows a higher amount of the main alloying elements of this steel.

4. Conclusion

The hot ductility of in situ melted and solidified low alloyed Cr-Mo steel was investigated. The region of low ductility was found to be between 750 and 850 °C having a minimum at 800 °C. This behavior is the result of deformation induced ferrite films surrounding the austenite grains, thus causing intergranular fracture if a stress is applied. Specimens without tensile deformation did not show any formation of ferrite. Solidification shrinkages through the melting process strongly affect the materials' cohesion, thus acting as internal notches when an external stress is applied. In both, deformed and undeformed specimens, hard spots appeared. These hard spots are caused by the dendritic solidification and the following macrosegregation of carbon into the Mn-rich regions during cooling.

Acknowledgments

Open access funding provided by Graz University of Technology. The research program of K1-MET, which has been financially supported within the Austrian competence centre program COMET by the Federal Ministry of Economy, Family and Youth; by the Federal Ministry for Transport, Innovation and Technology; by the provinces of Upper Austria, Styria and Tyrol; by the Styrian Business Promotion Agency; and by the Tiroler Zukunftsstiftung, has its focus on the modeling and simulation of metallurgical processes, including metallurgical raw materials and refractoriness with the goal of an optimal process control with respect to product quality, zero waste, and the minimization of energy and raw materials is acknowledged.

References

1. W.T. Lankford, Some Considerations of Strength and Ductility in the Continuous-Casting Process, *Metall. Trans. B*, 1972, **3**, p 1331–1357
2. M.M. Arıkan, Hot Ductility Behavior of a Peritectic Steel During Continuous Casting, *Metals*, 2015, **5**(2), p 986–999
3. R. Dippenaar, C. Bernhard, S. Schider, and G. Wieser, Austenite Grain Growth and the Surface Quality of Continuously Cast Steel, *Metall. Mater. Trans. B*, 2014, **45**, p 409–418
4. S. Ozturk, M.M. Arikan, and Y. Kacar, Effects of Nickel Coating of Mold Plates on Star Crack Defects, *Metall. Mater. Trans. B*, 2013, **44**, p 706–710
5. D.N. Crowther and B. Mintz, Hot Ductility of Steels and Its Relationship to the Problem of Transverse Cracking in Continuous Casting, *Int. Mater. Rev.*, 2010, **55**(3), p 168–196
6. B. Mintz, J. Lewis, and J.J. Jonas, Importance of Deformation Induced Ferrite and Factors Which Control Its Formation, *Materials Science and Technology*, 1997, **13**, p 379–388
7. B. Mintz, S. Yue, and J.J. Jonas, Hot Ductility of Steels and Its Relationship to the Problem of Transverse Cracking During Continuous Casting, *Int. Mater. Rev.*, 1991, **36**(1), p 187–220
8. B. Wang, Z.-P. Ji, W.-H. Liu, J.-C. Ma, and Z. Xie, Application of Hot Strength and Ductility Test to Optimization of Secondary Cooling System in Billet Continuous Casting Process, *J. Iron. Steel Res. Int.*, 2008, **15**, p 16–20
9. K.R. Carpenter, C.R. Killmore, and R. Dippenaar, Influence of Isothermal Treatment on MnS and Hot Ductility in Low Carbon, Low Mn Steels, *Metall. Mater. Trans. B*, 2014, **45**, p 372–380
10. B. Mintz, The Influence of Composition on the Hot Ductility of Steels and the Problem of Transverse Cracking, *ISIJ Int.*, 1999, **39**(9), p 833–855
11. H.G. Suzuki, S. Nishimura, and S. Yamaguchi, Characteristics of Hot Ductility in Steels Subjected to the Melting und Solidification, *Trans. ISIJ*, 1982, **22**, p 48–56
12. J. Clavo, A. Rezaeian, J. Cabrera, and S. Yue, Effect of the Thermal Cycle on the Hot Ductility and Fracture Mechanisms of a C-Mn Steel, *Eng. Fail. Anal.*, 2007, **14**(2), p 374–383
13. D. Djuric, C. Holler, M. Oberroither, B. Sonderegger, and C. Sommitsch, In Situ Melting Procedure for Determination of the High Temperature Properties of Steels, *Mater. Test.*, 2012, **54**(2), p 75–79
14. E. Kozeschnik, MatCalc version 6.00 (Database mc_fe_2.059). http://matcalc.tuwien.ac.at/. Accessed 2017
15. O. Caliskanoglu, S. Ilie, C. Beal, and C. Sommitsch, Hot Ductility Behavior of a Continuously Cast Steel During Solidification. In *STEELSIM 2013*, Technical University of Ostrava, Czech Republic (2013)
16. S. Koric, A. Murali, and B. Thomas, Elasto Visco-Plastic Model of Steel Solidification with Local Damage and Failure. In *Conference: International Symposium on Plasticity 2015 and Its Current Applications* (2015)

17. D.F. Majka, D.K. Matlock, and G. Krauss, Development of Microstructural Banding in Low-Alloy Steel with Simulated Mn Segregation, *Metall. Mater. Trans. A*, 2002, **33A**, p 1627–1637
18. G. Krauss, Solidification, Segregation, and Banding in Carbon and Alloy Steels, *Metall. Mater. Trans. B*, 2003, **34B**, p 781–792
19. E. Pickering and H. Bhadeshia, The Consequences of Macroscopic Segregation on the Transformation Behaviour of a Pressure-Vessel Steel, *J. Pressure Vessel Technol.*, 2014, **136**, p 031403. https://doi.org/10.1115/1.4026448
20. C. Voldrich, Cold Crackin in the Heat Affected Zone, *Weld. J.*, 1947, **26**, p 153–169